The application of graphene oxidized combining with decellularized scaffold to repair of sciatic nerve injury in rats

Qiaoling Wang [a,b,*], Jinlong Chen [c], Qingfei Niu [a,b], Xiumei Fu [b,d], Xiaohong Sun [b], Xiaojie Tong [b]

[a] College of Basic Medical Sciences, Shenyang Medical College, Shenyang 110034, China
[b] College of Basic Medical Sciences, China Medical University, Shenyang 110122, China
[c] Medical College, Shaoxing University, Shaoxing 312000, China
[d] College of Basic Medical Sciences, Chengde Medical College, Chengde 067000, China

ABSTRACT

This paper combined the decellularized scaffold of sciatic nerve of rats with graphene oxidized (GO), studied and facilitated the regeneration of sciatic nerve of rats, and provided the basis for the clinical application of nanomaterials. GO was prepared through improving Hammer's Method. Fourier Infrared Spectrum was used to scan and detect the functional groups in GO of sample by using the pellet method, the microcosmic morphological appearance of GO was observed by using the scanning electron microscope. The GO/decellularized scaffold were prepared and operation bridging of injured sciatic nerve was conducted by using the oscillation mixing method. BL-420F Biofunctional Experiment System was used to detect nerve action potential and the maximum tension value of muscles, and the fiber structure of nerve was observed under H-7650 Transmission Electron Microscope (TEM). Scanning electron microscope observed that GO presented a folded and curly single-layer sheet structure. It was soluble in water through ultrasound, brownish, the Fourier Transform Infrared Spectrometer detected the absorption peaks of carbonyl, hydroxy and carboxy, proving that the surface of GO material had many functional groups containing oxygen. Decellularized scaffold combining with GO was applied to repair injury of sciatic nerve, the nerve action potential, maximum tension value of muscle, wet weight value of gastrocnemius, thickness of gastrocnemius, thickness of myelin sheath and diameter of axon of the decellularized scaffold combining with GO group were obviously higher than the decellularized scaffold group and the self-rotating group, approaching to the normal value. All the data were represented by means ± standard deviation ($\bar{x} \pm s$) and processed by adopting SPSS 11.0 software. Comparisons among groups were analyzed by variance, and the comparison of two means was detected by student t. The detection level adopted $\alpha = 0.05$, when $P < 0.05$, it could be considered that there were significant differences. GO could combine with the biomaterial-decellularized scaffold to repair the injury of sciatic nerve and facilitate the regeneration of injured nerve. This provided new thoughts and theoretical & experimental bases for nanomaterials to be applied to clinic treatment of repair of nerve injury.

1. Introduction

Graphene is a new type of two-dimensional nanomaterials constituted by single-layer sheet carbon atoms, and its thickness is only the diameter size of one carbon atom (Rao et al., 2009). Graphene has very good transmittance, minimum resistivity and ultrastrong conductivity, the electrons on the surface can efficiently migrate, (Muhammad et al., 2017) and the connections among each carbon atom are extremely flexible (Halim et al., 2017; Rahman et al., 2017; Li et al., 2008; Allen et al., 2010; Barnard and Snook, 2008; Chen et al., 2004; Wang et al., 2009, 2011). But due to that the surface of graphene lacks functional groups, it is difficult to dissolve in solvent and easy to agglomerate. Graphene oxidized (GO) is a special derivative of graphene, its surface is rich in functional groups containing oxygen, such as epoxy group-CH(O)CH-, hydroxy-OH, and carboxy-COOH, which can change van der Waals force among sheet layers of GO and have

good biocompatibility and aqueous solution stability, the existence of functional groups is good for the modification of chemical functionalization, these factors make GO have received extensive attention, and be gradually applied to various fields, it also has more applications in aspects of cell imaging and drug delivery in the field of biomedicine (Luo et al., 2011; Barroso-Bujans et al., 2010; Sun et al., 2008; Jeong et al., 2008).

The long-distance peripheral nerve injury has caused permanent paralysis and sensory deprivation to its dominant position, bringing great burden and pressure to patients. Finding a suitable tissue material replacing nerves and recovering functions of limb of affected side as soon as possible have also become the hotspot for scientific research and clinical staff (Zhang et al., 2013; Cunha et al., 2010).

This research group transplants the decellularized scaffold - acellular nerve allograft (ANA) to rats, repair the long distance defect of sciatic nerve, the biocompatibility is better, which can facilitate the structure reconstruction of nerves and muscles and the recovery of motor function (Liu et al., 2013), and facilitate the repair of sciatic nerve injure. ANA is a three-dimensional scaffold which reserves extracellular matrix components, such as vessel of Schwann basilar membrane, epineurium and perineurium (Sun et al., 2004).

GO has good conductivity and absorbability, as to whether the decellularized scaffold (ANA) of sciatic nerve of rats can be combined with GO to facilitate nerve regeneration, there have been no relevant reports at present.

2. Material and methods

2.1. Materials

2.1.1. Reagents

95% ethanol (Shenyang Chemical Reagent Plant), barium chloride, sodium nitrate ($NaNO_3$), hydrogen peroxide, concentrated sulfuric acid (H_2SO_4), graphite powder, potassium permanganate ($KMnO_4$), potassium peroxydisulfate ($K_2S_2O_8$), phosphorus pentoxide (P_2O_5), Tris-HCl, Trit onX-100, PBS buffer, protease inhibitor (Aprotinin, Leupeptin, Pepstatin A), Dnase, Rnase and chloral hydrate dry powder were all purchased from Sigma Company, the penicillin and gentamycin were purchased from Sinopharm Group.

2.1.2. Instruments and equipment

JA1203 Electronic Balance, KQ3200E Ultrasonic Cleaner, JB-2 Timing Two-way Magnetic Heating Stirrer, D2F-6030 Vacuum Drying Oven, SHA-C Numerical Show Constant Temperature Waterbathing Oscillator, HH-2 Numerical Show Constant Temperature Oil-bathing, Centrifuge, S-3400N Scanning Electronic Microscopy, TU-1900 Double Beam UV-VIS Spectrophotometer, HJ90OB Digital pH Meter, HH-2 Numerical Show Constant Temperature Waterbathing Boiler, TENSOR27 Fourier Transform Infrared Spectrometer, 101-2AB Electrothermal Blowing Dry Box, 20-fold Operating Microscope, Microsurgical Instrument, Constant Temperature Oscillator, Micro Sample-adding Gun, BL-420F Biofunctional Experiment System, H-7650 Transmission Electron Microscope, Q3200E Ultrasonic Cleaner.

2.1.3. Experimental animals

65 healthy Sprague-Dawley (SD) rats of either gender with weights of 230–270 g (provided by Experimental Animal Center of China Medical University).

2.2. Experimental methods

2.2.1. Preparation of GO

2.2.1.1. Preoxidation. (1) 10 g graphite, 10 g $K_2S_2O_8$ and 10 g P_2O_5 were weighed, evenly mixed in solid state, and poured into the single ported round bottom flask; (2) mechanical stirring; (3) the measuring cylinder was used to take 30 ml H_2SO_4 (stir up); (4) reacted for 6 h in oil bath at 80 °C; (5) after the reaction completed, the wash bottle was used to add a little water into the round bottom flask (for the convenience to pour out the products), after stirring, evenly and respectively poured into 6 centrifuge tubes; (6) centrifugation was conducted for 15 min under 10,000 revolutions, after centrifugation, the supernatant was poured away, deionized water was added, after shaking evenly, this step was repeated until the supernatant became neutral; (7) after washing to neutrality, ethanol was used to wash for once (pour out and dry off); (8) the products were respectively poured onto two culture dishes, and put into the oven (60 °C) to dry off.

2.2.1.2. Oxidation. (1) 5 g dry preoxidation product and 4 g $NaNO_3$ were weighed, mixed evenly in solid state, and were poured into 3 flasks; (2) the round bottom flask was placed into ice-water bath (0 °C), and connected with the stirring device; (3) 184 ml concentrated H_2SO_4 was measured and slowly added to 3 flasks in stirring state, attention was paid to control the temperature below 5 °C; (4) 24 g $KMnO_4$ was measured and slowly add to the mixed solution for several times, stirred vigorously, the reaction temperature was controlled below 20 °C, this reaction reacted for 1 h in ice bath. Visible phenomenon: The solution turned from black to atrovirens. Kept stirring; (5) the ice bath was removed, the reaction was put into the oil bath pan (35 °C) to react for 30 min, take off, stirring was continued at normal temperature until the mixture became very viscous. (Standing for 5–7 d). Phenomenon: The solution turned from atrovirens to brown, and the viscosity was greatly increased.

2.2.2. Aftertreatment of GO oxide

2.2.2.1. The above-mentioned oxide was taken out. (1) 300 ml water was added to the three flasks in stirring state at room temperature; (2) the above-mentioned mixed solution was put into the oil bath pan (90 °C), Cand stir was continued for 15 min; (3) the mixed solution obtained after stirring was equally divided into 3 flasks.

2.2.2.2. Reoxidation. (1) 20 ml 30% H_2O_2 was measured and added to 1000 ml deionized water, H_2O_2 solution was respectively added to three beakers for several times (about 100 ml for each time), stirring while adding; (2) the mixed solution was poured into the centrifuge tube for centrifugation, the supernatant was poured away (after the supernatant was poured away, mixed solution can still be poured into the centrifuge tube to continue the centrifugation).

2.2.2.3. Washing. (1) 100 ml concentrated hydrochloric acid was measured to configure to 1000 ml solution, the above-mentioned product was washed for three times (pickling desalination), 1000 ml may be insufficient, which could be configured more as per the proportion. Continued to use the above-mentioned hydrochloric acid solution to wash until $BaCl_2$ detected that the supernatant had no white precipitates produced, i.e. no SO_4^{2-}; (2) the deionized water was used to continue to wash the above-mentioned product until the supernatant became neutral.

2.2.2.4. Drying. The above-mentioned product was put into the vacuum drying oven at 60 °C for 8 h.

2.2.3. Biocompatibility of GO

GO was ultrasonically prepared into liquid (0.2 mg/ml), 20 mg/kg GO was injected into abdominal cavities of 10 rats which were bred for 60 days.

2.2.4. Preparation of ANA

2.2.4.1. ANA was prepared by referring to hypotonic-detergent method of this research group. (1) 15 SD rats were narcotized by 10% chloral hydrate (350 mg/kg); (2) skin was prepared at 1 cm from the inferior border of buttock. The diameter was 2 cm. Under the sterile condition, the bilateral sciatic nerve trunks were bluntly dissected layer by layer and cut short, the sciatic nerves of rats were placed into the decellularized box (6-well cell culture plate); (3) tris-HCl, protease inhibitor and gentamycin were added to the box, constant temperature oscillation (40 rpm) was conducted for 4 days; (4) the liquid in the culture plate was poured away, and distilled water was used to wash for many times; (5) DNase and RNase stayed overnight at room temperature, (making DNA and RNA split); (6) 3% Triton-100, Tris-HCl, protease inhibitor and gentamycin were added to the culture plate, 40 rpm for 4 days; (7) washed for many times by distilled water; (8) PBS, gentamycin and penicillin were placed into the specimen box and store in refrigerator at 4 °C for standby application.

2.2.5. Preparation by GO combining with decellularized scaffold

2.2.5.1. Ultrasonic dissolution of GO. (1) 250 ml glass bottle was dried off under high pressure, 2 mg GO and 100 ml distilled water were added; (2) GO was ultrasonically dissolved and configured to 20 mg/ml GO solution as per serial dilution method.

2.2.5.2. Mixed preparation. The well prepared 10 ANAs were put into 20 mg/ml GO solution for 2 h, observed with election microscope for standby application.

2.2.6. Animal grouping

40 SD rats (weight of 230–270 mg) of either gender and random grouping. 10 for normal control group, 10 for GO combining with ANA experiment group (GO20 group), 10 for ANA group (blank group), and 10 for self-rotating transplant at group.

2.2.7. Surgical transplantation of scaffold

Firstly, 10% chloral hydrate was used for anaesthesia, 350 mg/kg, sterile intraperitoneal injection, lied prostrate, fixed, the operation side was the right side, the skin was incised at 1.5 cm from the inferior border of buttock and 2 cm from the posterior midline, the buttock muscles and posterior thigh muscles appeared, the fascial space was found, the sciatic nerve trunk was separated, during operation, the site 5 mm from the inferior border of piriformis muscle was selected, about 8 mm of sciatic nerve trunk was cut off, natural retraction was allowed, the two defect ends reached 10 mm, the prepared ANA and GO/ANA were used to make the autologous sciatic nerve transection and reversion transplant to the defect site of nerve. Microscopically, 10–0 microscopic operative suture was used for suturing, iodophor was used to disinfect the wound surface, and 5–0 microscopic operative suture was used to suture skins and muscles. The operation conducted by normal control group only revealed sutured muscles and skins behind the sciatic nerve on the right side. Bred in cages for each group after operation.

2.2.8. Electrophysiology determination of nerves and muscles

BL-420F Biofunctional Experiment System produced by Chengdu Techman Software Co. Ltd. was used to determine the sciatic nerve action potential. Recording method: The rat was narcotized, gradually revealing the sciatic nerve trunks of operation sides. Separated to nerve entry point to muscle along the trunk. The tip of acupuncture needle was bended and made into hook-type electrodes to be respectively placed at the proximal end and distal end of transplant, stimulated for the proximal end and recorded for the distal end. Muscular tension sensor of biofunctional experiment system was used to determine the maximum muscular strength of gastrocnemius (Ishaq and Jafri, 2017). The site of Achilles's tendon was separated, a rope (surgical suture) was tied, broken and separated to politeal fossa, reserve innervation was reserved, and the fascia connection with other muscles was bluntly separated. The innervation between shank and other muscles of buttock was cut off.

2.2.9. Wet weight ratio determination of gastrocnemius

The gastrocnemius on uninjured (left) side and that on the operation (right) side were taken, the wet weight was measured by analytical balance, and the specific value of gastrocnemius between operation side and uninjured side was obtained.

2.2.10. The shape of the transplanted sciatic nerve scaffold was observed under electron microscope

2.2.10.1. Specific steps. (1) For animals having undergone perfusion by normal saline, the middle sections of transplants in each group were taken, 25% glutaraldehyde was used for pre-fixation at 4 °C for at least 2 h, and buffer solution was used to wash for 3 times at room temperature; (2) 1% osmium tetroxide solution was used for post-fixation at 4 °C for 2 h, and buffer solution was used to wash for 3 times at room temperature; (3) gradient alcohol was used for dehydration, replaced by acetone; (4) embedded by epoxy resin, ultrathin section; (5) uranyl acetate and lead citrate were used for dyeing, and ultramicroscopic structure was observed by H-7650 Transmission Electron Microscopy; (6) MetaMorph/DP10/BX41 Image Analysis System was used to analyze the quantity of regenerative nerve fibers, thickness of myelin sheath and diameter of neurite.

2.3. Statistical treatment

SPSS11.0 statistical software package was adopted to conduct data processing and one-way analysis of variance, intergroup differences had statistical significance, then pairwise comparison was conducted. The detection level adopted $\alpha = 0.05$, when $P < 0.05$, it could be considered that there are significant differences.

3. Results

3.1. Preparation of GO

3.1.1. Result and representation of GO

3.1.1.1. The method to obtain GO. The modified Hummers Method was used to obtain GO after graphite had been oxidized and dried off shown in Fig. 1. The solid sheet shape of GO was shown in Fig. 2.

3.1.1.2. Ultrasonic dissolution. 2 mg solid GO was measured to be placed into 250 ml glass bottle and dried off under high pressure,
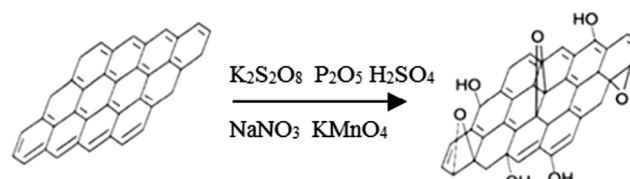

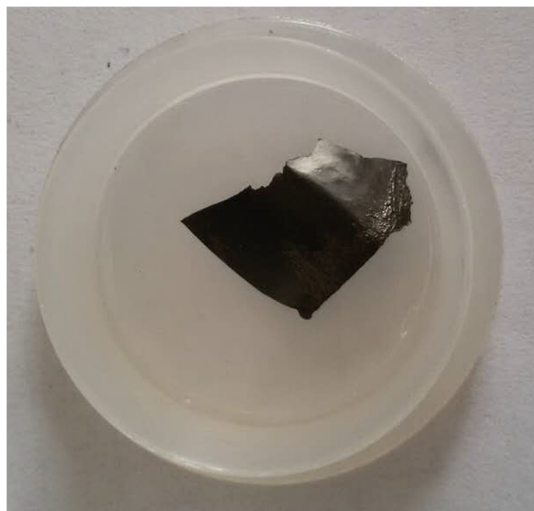**Fig. 1.** Schematic diagram for GO preparation from graphite by modified Hummers method.

Fig. 2. Solid sheet shape of GO.

100 ml high-pressure distilled water was measured. GO ultrasonically dissolved in water was brown.

3.1.1.3. Observation under scanning electron microscope. The micromorphology of GO was observed in scanning electron microscope. Through the scanning of electron microscope and acceleration voltage of 20 kV, magnified by 10,000 times, GO which presented
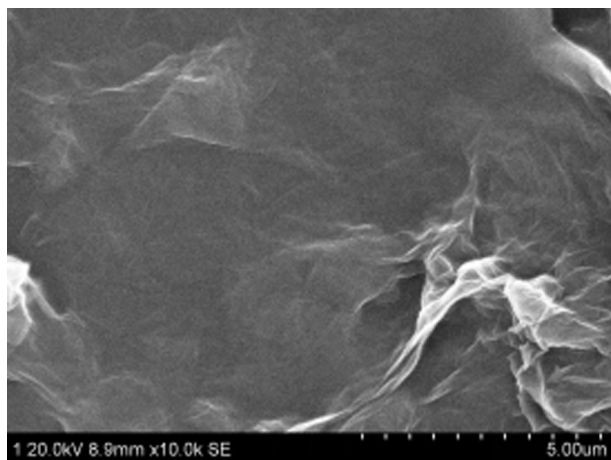

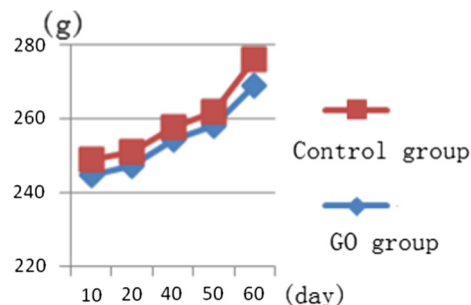**Fig. 3.** GO SEM graph 8.9 mm × 10.0 k.

Fig. 5. Weight change condition of control group and GO given group.

the single-layer sheet structure and plicated and curly morphology features was observed shown in Fig. 3.

3.1.1.4. Analysis by Fourier transform infrared spectrometer (FT-IR). In the infrared absorption spectrum of Fig. 4, it could be seen that there were many oxygen-containing groups on the surface of GO material, wherein the absorption peak of characteristic of O—H appeared at 3240 cm^{-1}, the absorption peak here was relatively wide, the absorption peaks at 1728 cm^{-1} and 1644 cm^{-1} were caused by C = 0 stretching vibration and the O—H vibration in C—OH functional group.

3.2. Observation on biocompatibility

3.2.1. General situation

No toxic reaction was seen, the weight had increased, no death phenomenon was seen, the mental state was good, active, the appetite was good. Weight change condition of each group was shown in Fig. 5.

In order to prove the toxicity performance of GO on experimental rats, the liver function of rats was tested through haematology. Rats of the control group and GO group were narcotized and executed in the 10th, 20th, 40th and 60th day, the reserved blood was drawn, and biochemical examination was conducted. The result showed that, compared with the control group, alanine aminotransferase and aspartate transaminase had no obvious differences, the differences were within the scope of reference value shown in Fig. 6. This explained that GO had no obvious toxic effect on organisms.

3.2.2. Postoperative observation

After operation, the involution of rat skin at operation side of each group was smooth, the healing was good, no inflammation
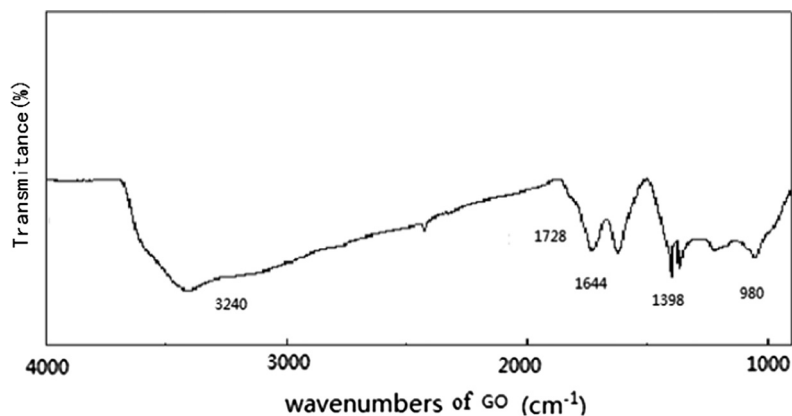
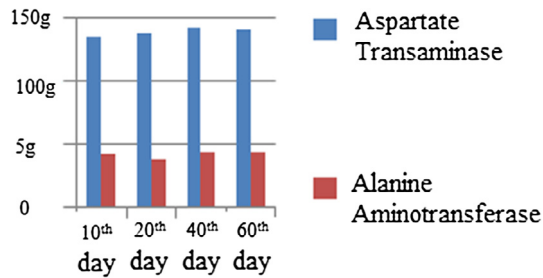

Fig. 4. FT-IR Analysis diagram.

Fig. 6. Levels of alanine aminotransferase and aspartate transaminase in blood of rats.

and inflammatory exudation were seen in Fig. 7, the mental state and dietetic activity had no abnormality.

Besides the normal control group, the lower limbs of rats at operation side in each group were paralyzed, overbending of hips, knees and toes occurred when they were unable to normally stretch the hips, knees and toes. In the 1st week after operation, the skin incision was normally healed up, in the 3rd-4th weeks after operation, denervated muscle atrophy appeared. In the 11th week, the muscle strength had recovery, the action of back step had force, the toes can slightly separated but still hadn't reached the standard. The sampling had seen that transplants of each group of rats slightly had adhesion with peripheral tissues and were easy to separate.

3.3. Electroneurophysiological determination

3.3.1. Compound action potential

The action potential led by two electrodes was biphase compound action potential. The result showed: In the 11th week after transplantation, the determination of regeneration nerve by electrophysiology found that the difference of numerical values of compound action potential also showed the recovery condition of internal nerve fibers (Sarfraz et al., 2017), the good regeneration nerve action potential was close to the normal value shown in Table 1. The peak-to-peak value of nerve action potential in GO20 group was obviously higher than the blank group and the self-rotating group ($P < 0.05$) shown in Fig. 8, which had statistical significance.

3.3.2. Maximum tension of muscles

The muscle tension transducer was used to measure the maximum value and mean value of muscle tension of affected side in each group. The ratio of the maximum values of muscle tension between affected side and normal side in GO20 group had greatly exceeded the blank group and the self-rotating group shown in Fig. 9, all the P values were less than 0.05 shown in Table 2.

Table 1
Peak-to-peak value ratio between affected side and normal side of action potentials in each group.

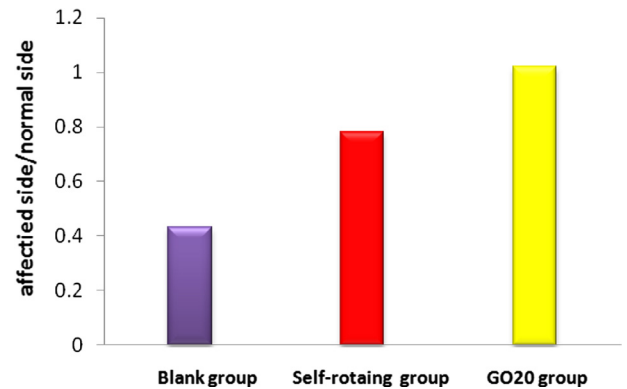| x̄	Affected side/ normal side	F	P
Blank group	0.4300 ± 0.0372		All the P values of each
Self-rotating group	0.7821 ± 0.0578	528.78	group through pairwise
GO20 group	1.0197 ± 0.0161		comparison were less than 0.05

Fig. 8. Peak-to-peak value ratio between affected side and normal side of sciatic nerve action potentials in each group.

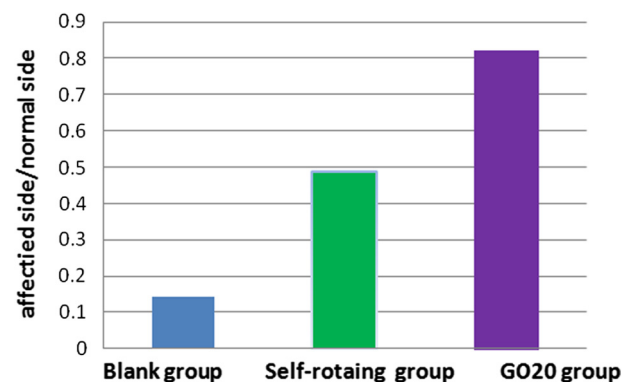**Fig. 9.** Muscle tension ratio between affected side and normal side in each group.

3.3.3. Wet weight ratio of gastrocnemius

The wet weight ratio of gastrocnemius could reflect the rehabilitation level of muscles on the affected side. The wet weight ratio of
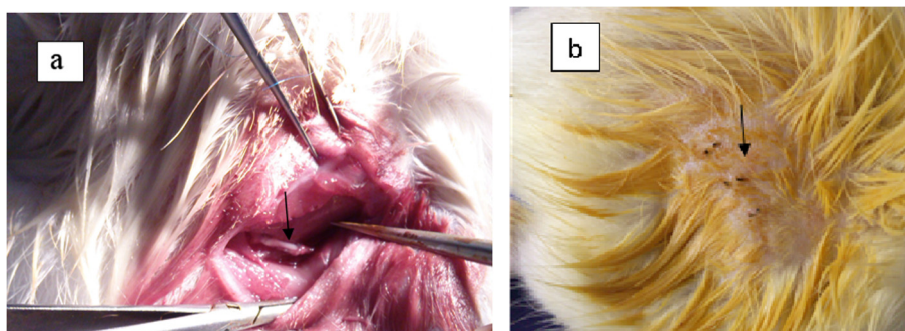

Fig. 7. (a) After intraoperative anastomosis; (b) skin incision after operation.

Table 2
Gastrocnemius tension ratio between affected side and normal side in each group.

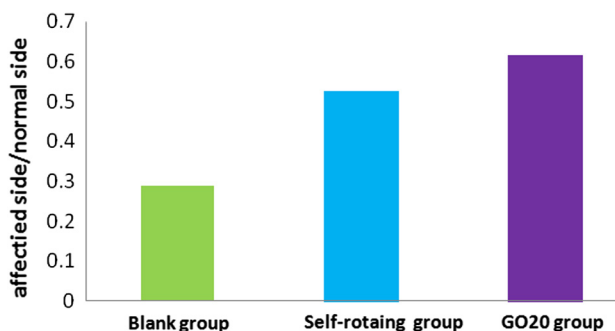|	Affected side/normal side	F	P
Blank group	0.1414 ± 0.0144		All the P values of each group through pairwise comparison were less than 0.05
Self-rotating group	0.4878 ± 0.0246	3153.982	
GO20 group	0.8208 ± 0.0167		

Fig. 10. Comparison of wet weight ratio of gastrocnemius in each group.

Table 3
Wet weight ratio of gastrocnemius in each group.

Group	Wet weight ratio	F	P
	Affected side/normal side		
Blank group	0.2877 ± 0.0070		All the P values of each group through pairwise comparison were less than 0.05
Self-rotating group	0.5257 ± 0.020	408.704	
GO20 group	0.6145 ± 0.0403		

gastrocnemius in GO20 group was significantly higher than the blank group and the self-rotating group shown in Fig. 10, and the difference had statistical significance (P < 0.05) shown in Table 3.

3.3.4. Observation under electron microscope

H-7650 Transmission Electron Microscopy magnified to conduct ultrastructure observation in which the decellularized scaffold was in the shape of onion skin without components of organelle. Through scaffold bridging, the myelin sheath of GO20 group thickened, tending to be completely close to the normal group, there were axon growing and quantity increase of myelinated fibers, the Schwann cells were visible, but the diameter of nerve fiber was less than the normal group, and was bigger than the thickness of myelin sheath of the self-rotating group, the diameter was large shown in Fig. 11. The thickness of myelin sheath in the blank group was uneven and inferior to the nanomaterial combining with decellularized scaffold group, the recovery condition of the nanomaterial combining with decellularized scaffold group was obviously higher than the blank group.

The recovery of thickness of myelin sheath and diameter of axon of GO20 group was significantly higher than the self-rotating group and the blank group, P < 0.05, having statistical significance shown in Table 4. Compared with the normal group, it still hadn't become normal.

4. Discussion

Nanometer is a length unit that is equal to 1/10 hundred million meters, make an attempt to form new substances within the scale range of nanometer. Nanotechnology is an emerging interdisciplinary science which is developing rapidly. Graphene is a famous nanomaterial discovered by Professor Gein et al. from University of Manchester of UK in 2004, it is in single-layer sheet shape with the diameter thickness of one carbon atom (Novoselov et al., 2004). Graphene has very good transmittancy, minimum resistivity, ultrastrong conductivity, the electrons on the surface can efficiently migrate, and the connections among each carbon atom is very flexible (Li et al., 2008). The application of graphene to electrochemical immunosensor for antigen detection has greatly improved the sensitivity of detection, the 0.02 ng/ml α-fetoprotein in human serum can be detected through the sensor constructed by graphene and carbon nanotube (Song et al., 2012; Jia et al., 2012; Wang et al., 2013).

GO is the derivative of graphene with a huge specific surface area, thus having good absorption effect. Meanwhile, as it has a large amount of functional groups, such as hydroxyl, epoxy group and carbonyl, which overcome the defects of easy agglomeration and difficult hydrolysis of graphene, thus having good biocompatibility and aqueous solution stability. It also can conduct modification of chemical functionalization. There are scientific researchers having ever used GO to load antineoplastic drugs of Doxorubicin and Oridonin, making side effect reduction of antineoplastic drug and targeted drug delivery become possible (Wu, 2013; Ni et al., 2011, 2013). This shows the scientific value and potential of nanomedicine, becoming a hotspot of research nowadays.

This experiment prepares GO through the modified Hummers Method with graphite undergoing the treatment of strong acid and oxidizing agent, the structure is single-layer sheet without phenomenon of agglomeration, the surface of GO prepared by Fourier Transform Infrared Spectrometer is rich in oxygen-containing groups. Being rich in a large quantity of oxygen-containing groups on the surface makes the van der Waals force among layers strengthen, become difficult to form agglomeration, and easy to dissolve in water under the power of ultrasound, it is easier to be modified than graphene.

Nanobiomedicine is an important branch of nanoscience, the series of peculiar properties and functions of nanostructure have important application values for the development in fields of life science and human health. Scientific research personnel use nanomaterials to fabricate scaffold for tissue engineering to facilitate cell differentiation, tissue regeneration, peripheral nerve regeneration and repair of central nerve injury (Cho and Borgens, 2012; Fraczek-Szczypta, 2014; Li et al., 2011a,b,c; Misraa et al., 2010; Okamoto and John, 2013).

Graphene is a new type of two-dimensional nanomaterial, there have been scientific research personnel applying graphene to cure tumor and cancer, someone has ever researched its toxicity and antibacterial property on cells (Lu, 2002; Hu et al., 2010; Huang and Chen, 2009; Hull et al., 2007; Goyal et al., 2013). Graphene is nontoxic and has bacteriostasis function. GO is the derivative of graphene, the functionalized graphene has the function of facilitating the growth of neuritis (Akhavan et al., 2012; Zhang et al., 2010; Tu et al., 2013). This paper combines the functionalized graphene with the decellularized scaffold to discuss the function on nerve regeneration.

In this experiment, GO nanomaterial has satisfying biocompatibility, which can combine with the decellularized scaffold of sciatic nerves of rats for bridging of 100 mm injured sciatic nerve. In the 11th week after operation, compare the action potentials of regeneration nerves, diameter of regenerative nerve fiber axon,
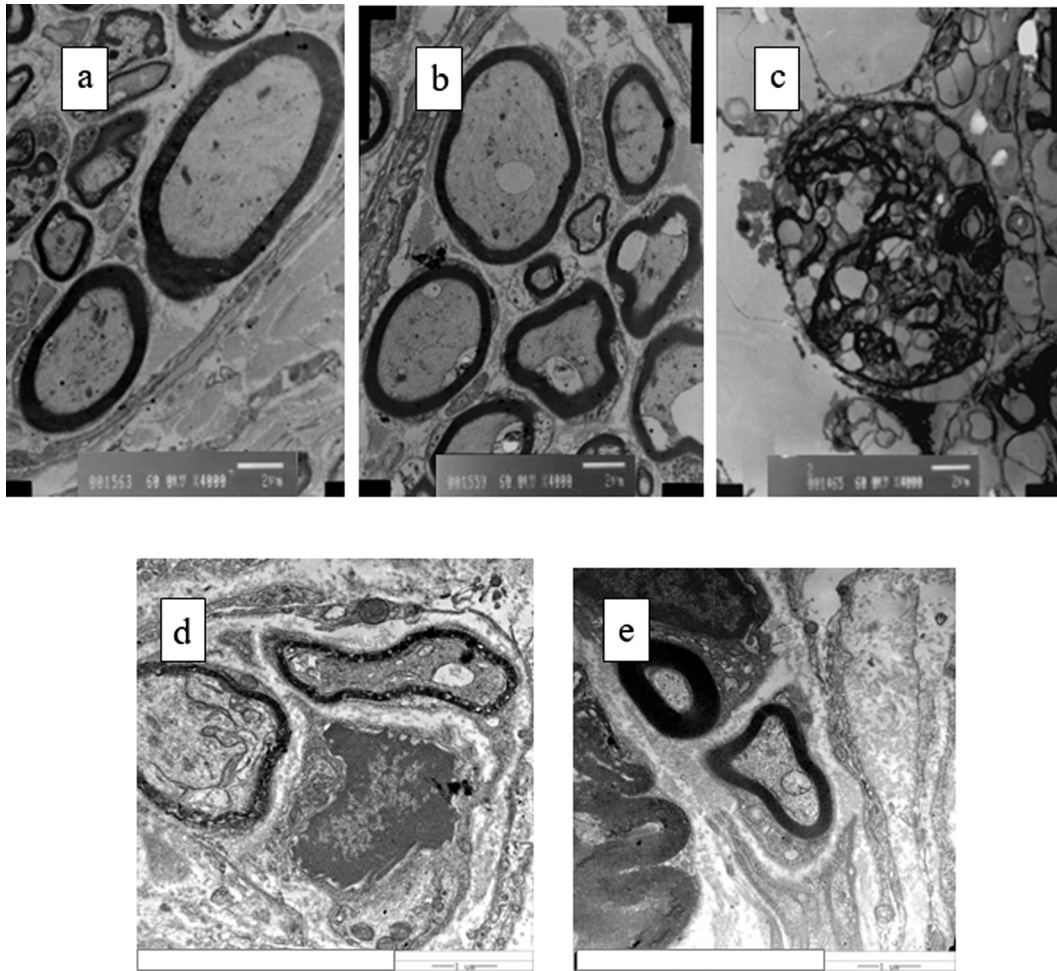
Fig. 11. (a) Transmission electron microscope photos of sciatic nerve; (b) normal control group; (c) GO20/ANA group Decellularized scaffold/GO; (d) blank group; (e) self-rotating group.

Table 4
Data on thickness of myelin sheath and diameter of axon of sciatic nerve in each group.

	Thickness of myelin sheath (μm)	Diameter of axon (μm)	p
Self-rotating group	0.4512 ± 0.0249	1.7522 ± 0.1181	All the P values of each
Blank group	0.2523 ± 0.0328	2.5194 ± 0.2604	group through
GO20 group	0.9047 ± 0.0034	10.0061 ± 0.0533	pairwise
Normal control group	1.0379 ± 0.0038	10.8571 ± 0.0790	comparison were less than 0.05

thickness of myelin sheath and the maximum tension recovery condition of axon growing towards the distal end to dominate the posterior muscular group of calf in the nanomaterial group, blank group and self-rotating group. Considering the individual differences, compare the recovery condition of affected side with the autologous normal side, and compare the ratios among each group. Through single factor comparison and variance analysis, the intergroup pairwise comparison has significant difference, P value is less than 0.05, having statistical significance. The peak-to-peak value of sciatic nerve action potentials by nanomaterial group combining with decellularized scaffold group is obviously higher than the blank group and the self-rotating group, the ratio is close to 1, nanomaterial combining with decellularized scaffold

is like plating a layer of conducting material outside the decellularized. GO has very strong conductivity, making the conductivity of combined decellularized scaffold strength, facilitating the regeneration of axon within scaffold, the conduction of action potentials and the regeneration of nerve. Meanwhile, the thickness of myelin sheath and the diameter of axon are obviously higher than the blank group and the self-rotating group, the regeneration speed of sciatic nerve of nanomaterial group is obviously quicker than other groups. The quicker the regeneration speed of sciatic nerve, the quicker the calf muscle that extends to domination, making the denervated muscles recover the motor ability earlier (Atta et al., 2017). The muscular movement makes the atrophy produced by loss of motor gradually rehabilitate, the tension of muscles strengthen, forming good development trend of rehabilitation. In the experiment, we find that the recovery of sciatic nerve action potentials, thickness of myelin sheath, size of diameter of axon and muscular tension of dominated muscles present a directly proportional relationship.

As GO nanomaterial has ultra-strong absorbability, it can be modified into the nanomaterial with more excellent performance, if it is modified by titanium dioxide, its stability in liquid can be improved, and the specific surface area can be increased; it also can be modified into the nanomaterial with magnetic function by amino ferroferric oxide. In this experiment, GO and the modified GO can be loaded with drugs such as Vitamin B1 and Vitamin P. If nanomaterial loaded with drugs recombines with the decellularized scaffold to cure long-distance sciatic nerve injury, it can

increase the concentration of local plasma concentration, whether it can facilitate the repair of nervous tissue quicker needs to be further verified by the following experiment.

5. Conclusions

This experiment had verified that GO nanomaterial could combine with allogeneic sciatic nerve decellularized scaffold to facilitate nerve regeneration. The sciatic nerve action potentials, thickness of myelin sheath, diameter of axon and dominated muscle rehabilitation level of the nanomaterial group were significantly higher than the blank group and the self-rotating group.

References

Akhavan, O., Choobtashani, M., Ghaderi, E., 2012. Protein degradation and RNA efflux of viruses photocatalyzed by grapheme-tungsten oxide composite under visible light irradiation. Phys. Chem. C 116, 9653–9659.

Allen, M.J., Tung, V.C., Kaner, R.B., 2010. Honeycomb carbon: a review of graphene. Chem. Rev. 110, 132–145.

Atta, A., Mustafac, G., Sheikh, M.A., Shahid, M., Xiao, H., 2017. The biochemical significances of the proximate, mineral and phytochemical composition of selected vegetables from Pakistan. Matrix Sci. Pharma 1 (1), 06–09.

Barnard, A.S., Snook, I.K., 2008. Thermal stability of grapheme edge structure and grapheme nanoflakes. Chem. Phys. 128, 09470–09477.

Barroso-Bujans, F., Cerveny, S., Verdejo, R., et al., 2010. Permanent adsorption of organic solvents in graphite oxide and its effect on the thermal exfoliation. Carbon 48 (4), 1079–1087.

Chen, G.H., Weng, W.G., Wu, D.J., et al., 2004. Preparation and characterization of grahphite nanosheets from ultrasonic powdering technique. Carbon 42, 753–759.

Cho, Y., Borgens, R.B., 2012. Polymer and nano-technology applications for repair and reconstruction of the central nervous system. Exp. Neurol. 233, 126–144.

Cunha, C., Panseri, S., Antonini, S., 2010. Emerging nanotechnology approaches in tissue engineering for peripheral nerve regeneration. Brain A J. Neurol. 133 (11), 50–59.

Fraczek-Szczypta, A., 2014. Carbon nanomaterials for nerve tissue stimulation and regeneration. Mater. Sci. Eng. C 34, 35–49.

Goyal, M. et al., 2013. Analgesic and anti-inflammatory studies of cyclopeptide alkaloid fraction of leaves of Ziziyphus num-mularia. Saudi J. Biol. Sci. 20 (4), 365–371.

Halim, A.N.I., Huyap, F., Hamid, A.T.T.H., Halim, A.K.B., Hamid, A.A.A., 2017. In silico binding interactions of dehalogenase (Dehe) with various haloalkanoic acids. Galeri Warisan Sains 1 (1), 04–06.

Hu, W., Peng, C., Luo, W., et al., 2010. Graphene-based antibacterial paper. ACS Nano 4, 5731–5736.

Huang, Y., Chen, Y.S., 2009. Functionalization of graphene and their application. Sci. China, Ser. B 30, 887–896.

Hull, M.S., Kennedy, A.J., Steevens, J.A., et al., 2007. Release of metal impurities from carbon nanomaterials influences aquatic toxicity. Environ. Sci. Technol. 387 (2), 637–648.

Ishaq, S., Jafri, S., 2017. Biomedical importance of cocoa (Theobroma cacao): significance and potential for the maintenance of human health. Matrix Sci. Pharma 1 (1), 01–05.

Jeong, H.K., Lee, Y.P., Lahaye, R.J., 2008. Evidence of graphitic AB stacking order of graphite oxides. J. Am. Chem. Soc. 130 (4), 1362–1366.

Jia, C.J., Wang, L.J., Du, Z.Z., 2012. Study on an electrochemical immunosensor based on graphene/chitosan/carbon nanotube detection of alpha fetal protein. Chemistry 75 (11), 1048–1051.

Li, H., Wei, Q., He, J., et al., 2011a. Electrochemical immunosensors for cancer biomarker with signal amplication based on ferrocene functionalized iron oxide nanoparticles. Biosens. Bioelectron. 26 (8), 3590–3595.

Li, N., Zhang, X., Song, Q., et al., 2011b. The promotion of neurite sprouting and outgrowth of mouse hippocampal cells in culture by grapheme substrates. Biomaterials 32, 19–27.

Li, N.W., Zhen, M.B., Chang, X.F., et al., 2011c. Preparation of magnetic CoFe2O4 – functionalized grapheme sheets via a facile hydrothermal method and their adsorption properties. J. Solid State Chem. 184, 953–958.

Li, X.L., Wang, X.R., Zhang, L., et al., 2008. Chemically derived, ultrasmooth graphene nanoribbon semiconductors. Science 319, 1228–1232.

Liu, G.B., Cheng, Y.X., Feng, Y.K., et al., 2013. Study on the potentiality of adipose-derived stem cells in repairing peripheral nerve injury. Chin. J. Neuroanat. 29 (1), 61–64.

Lu, S.B., 2002. The position and application of nanotechnology in the development of life science. Acta Acad. Med. Sin. 24, 111–113.

Luo, Y.B., Shi, Z.G., Gao, Q., et al., 2011. Magnetic retrieval of graphene: extraction of sulfonamide antibiotics from environmental water samples. J. Chromatogr. A 1218, 1353–1358.

Misraa, S.K., Ansari, T.I., Valappil, S.P., 2010. Poly (3-hydroxybutyrate) multifunctional composite scaffolds for tissue engineering applications. Biomaterials 31, 2806–2815.

Muhammad, G., Rashid, I., Firyal, S., Saqib, M., 2017. Successful treatment of idiopathic generalized subcutaneous emphysema in kajli a ram by large bore injection needle. Matrix Sci. Medica 1 (1), 01–02.

Ni, Y., Zhang, F., Kokot, S., 2011. Functionalized grapheme oxide as nanocarrier for loading and delivery of ellagic acid. Curr. Med. Chem. 18, 4503–4512.

Ni, Y.N., Zhang, F.Y., Kokot, S., 2013. Graphene oxide as a nanocarrier for loading and delivery of medicinal drugs and as a biosensor for detection of serum albumin. Anal. Chim. Acta 769 (6), 40–48.

Novoselov, K.S., Gem, A.K., Morozov, S.V., et al., 2004. Electric field in atomically thin carbon films. Science 306, 666–669.

Okamoto, M., John, B., 2013. Synthetic biopolymer nanocomposites for tissue engineering scaffolds. Prog. Polym. Sci. 38, 1487–1503.

Rahman, A.S., Kahar, A.A., Mansor, A., Murni, D.L., Hussin, A., Sharifudin, A.S., Hun, T.G., Rashid, A.N.Y., Othaman, M.A., Long, K., 2017. Identification of potential indigenous microbe from local fermented vegetables with antimicrobial activity. Galeri Warisan Sains 1 (1), 01–03.

Rao, C.N.R., Biswas, K., Subrahmanyam, K.S., et al., 2009. Graphene, the new nanocarbon. Mater. Chem. 19, 2457–2469.

Sarfraz, M., Ashraf, Y., Ashraf, S., 2017. A review: prevalence and antimicrobial susceptibility profile of listeria species in milk products. Matrix Sci. Medica 1 (1), 03–09.

Song, Y.P., Feng, M., Zhan, H.B., et al., 2012. Applications of graphene nanocomposites in electrochemical biosensors. Prog. Chem. 24 (9), 1665–1673.

Sun, H.Z., Tong, X.J., Cao, D.S., et al., 2004. Preparation of acellular nerve allografts and analysis of their components. Prog. Anat. Sci. 10, 106–108.

Sun, X., Liu, Z., Weisher, K., et al., 2008. Nano-graphene oxide for cellular imaging and drug delivery. Nano Res. 1 (3), 203–212.

Tu, Q., Pang, L., Wang, L.L., et al., 2013. Biomimetic choline-like graphene oxide composites for neurite sprouting and outgrowth. ACS Appl. Mater. Interfaces 5, 13188–13197.

Wang, Y., Li, Y.M., Tang, L.H., et al., 2009. Application of graphene-modified electrode for selective detection of dopamine. Electrochem. Commun. 11, 889–892.

Wang, C., Feng, C., Gao, Y.J., et al., 2011. Preparation of a grapheme-based magnetic nanocomposite for the removal of an organic dye from aqueous solution. Chem. Eng. J. 173, 92–97.

Wang, G.F., Zhu, Y.H., Chen, L., et al., 2013. Applications of functional nanomaterials in electrochemical immunosensor. Chin. J. Anal. Chem. 41 (4), 608–615.

Wu, S.L., 2013. Study in graphene oxide loaded with doxorubicin and effect of graphene oxide loaded with doxorubicin on multiple myeloma cell. Shandong University.

Zhang, Y., Ali, S.F., Dervishi, E., et al., 2010. Cytotoxicity effects of graphene and single-wall carbon nanotubes in neural phaeochromocytoma-derived PC12 cells. ACS Nano 22, 3181–3186.

Zhang, Y.D., Wang, X.M., Huang, G.Z., 2013. Research progress of peripheral nerve injury repair. Chin. J. Injury Repair Wound Healing: Electron. Ed. 8, 210–213.